Effect of a dielectric medium on spontaneous radiation in a uniform magnetic field: Higher harmonics and the helical Čerenkov effect

Josip Šoln
Harry Diamond Laboratories, Adelphi, Maryland 20783-1197
(Received 2 March 1992)

The mechanism of the spontaneous emission in a uniform magnetic field with a dielectric medium is being studied. The actual process can be divided into two branches: a vacuum branch and a Čerenkov branch. In the limit of vanishing matter density, a vacuum branch is the only one that remains. For each of these two branches, we derive general expressions for angular energy and power distributions with the corresponding spectra. For the Čerenkov branch, however, we deduce that a new effect, a helical Čerenkov effect, exists in a dielectric medium. This effect, unlike the ordinary Čerenkov effect, depends on the radius of curvature of the electron trajectory, measured in a plane perpendicular to the direction of the electron guiding center. Furthermore, for an index of refraction n that is independent of the radiation angle and also is a slowly varying function of the radiation frequency, the spontaneous emission from spiraling electrons may go into a large number of harmonics for either of the two branches. As compared to a vacuum, the effect of the dielectric medium is to increase the overall energy emission.

PACS number(s): 41.60.Bq, 32.60.+i, 32.80.Wr

I. INTRODUCTION

As is well known, the presence of a dielectric medium can significantly alter a mechanism of electron radiation as compared to a vacuum [1]. For example, it was found that the radiation resulting from electrons interacting with a static wiggler magnet in a dielectric medium can go through two branches: a vacuum branch and a Čerenkov branch [2]. Not surprisingly, the same thing should be true for radiation in a medium caused by other forces on the electron rather that just the ones coming from a wiggler magnet. Indeed, we find that in a medium the spontaneous emission from spiraling electrons caused by a uniform magnetic field can also go through vacuum and Čerenkov branches.

The spontaneous emission in a dielectric medium from electrons moving on helical orbits in a uniform magnetic field [3] is a good example for deducing some general characteristics of spontaneous emission in a medium. First, we learn that generally, a new effect, a helical Čerenkov effect, should exist in a dielectric medium. This effect, unlike the usual Čerenkov effect, depends on the radius of curvature of the electron trajectory; for example, for higher-kinetic-energy electrons, say, 1 MeV and above, it is strongest when the radius of curvature becomes comparable to the radiation wavelength. Furthermore, we find that as long as index of refraction n is a slowly varying function of the radiation frequency, the spontaneous emission may go into a large number of harmonics for either of the two branches.

Specifically, in this article, we derive the expressions for energy and power spectra and the corresponding energy and power angular distributions of spontaneous emission in a dielectric medium from electrons in a uniform magnetic field. This is done by utilizing the customary definition of the Bessel functions which, in turn, allows us to expand the electron current density into a Fourier-like series [3]. It is from the expression of a power spectrum that we deduce a new helical Čerenkov effect whose existence, however, depends more on the curvature than the nature of the electron trajectory. Furthermore, from the expression for angular energy distribution, we conclude that the harmonic emission is clearly identifiable only for the isotropic dielectric medium whose index of refraction n is a very slowly varying function of the radiation frequency.

When this is the case, we can actually evaluate analytically the total, over kinematically allowed radiation frequencies, spontaneously emitted energy distribution at a sufficiently small radiation angle, provided that the fundamental and higher-harmonic frequencies are much smaller than the first resonance frequency of the dielectric medium. In these evaluations, the spontaneous emission into higher harmonics is assumed to be negligible beyond some sufficiently high harmonic number [3]. From the practical point of view, this means that appreciative amounts of energy are emitted only into a finite number of harmonics, which, in principle, should be true for any radiation angle, again provided that all the harmonic radiation frequencies are much smaller than the first resonance dielectric frequency. Of course, when some of the radiation frequencies are close to a resonance frequency of the medium, index of refraction n becomes strongly dependent on the radiation frequency and the evaluations of energy spectra and angular energy distributions generally can be carried out only through numerical methods, except perhaps when a simple model is assumed for the dielectric function [4].

For the sake of completeness, we mention another well established and important radiation by relativistic electrons in a uniform magnetic field, the spontaneous synchrotron radiation. It occurs in a vacuum when the elec-

tron is moving in a uniform circular motion in a plane perpendicular to the direction of the uniform magnetic field with electron radiating in the direction of the electron velocity. The expression for the angular-spectral energy distribution that is used quite often in calculations was obtained by Schwinger [5] in 1949, although, under the terminology of circular motion, similar results have been obtained already in 1912 by Schott [6].

Taking into account that, on one hand, the uniform magnetic field plays a rather important role in radiation generation and, on the other hand, that the helical Čerenkov effect and the spontaneous harmonic emission in a medium may be of significant practical interest, we feel, is sufficient justification for studying the spontaneous electron emission in a dielectric medium with a uniform magnetic field.

In Sec. II the general multiphoton formalism suitable for treating the spontaneous emission in a dielectric medium with finite interaction time is briefly described. Here the general expressions for energy and power spectra as well as angular energy and power distributions in a dielectric medium are given. In Sec. III, the new helical Čerenkov effect is derived, compared with the usual Čerenkov effect, and we discuss the electron energies and radiation frequencies for which it should be possible to observe it. Here, also, the specifics of the higher-harmonic emission in the dielectric medium are elaborated. The results are discussed and summarized in Sec. IV.

In what follows, for the sake of simplicity, we shall assume that the medium is nonmagnetic so that the magnetic permeability μ satisfies $\mu=1$. Then magnetic fields $\mathbf{B}$ and $\mathbf{H}$, related by $\mathbf{B}=\mu\mathbf{H}$, are the same.

II. MULITPHOTON DESCRIPTION OF SPONTANEOUS EMISSION IN A MEDIUM OVER A FINITE INTERACTION TIME

Here we modify the S matrix, describing the spontaneous emission in a medium [1,2] from an infinite interaction time [1,2] to a finite interaction time S matrix. To do that we utilize the finite interaction time T action integral [3] in terms of the free photon potential and the conserved electron current density as

$$I(A,j;T)=I(A,j;T;+)+I(A,j;T;-)\ ,$$
$$I(A,j;T;+)=\int_{-T/2}^{T/2}dt\int d^3x\ A_\mu(x;+)j^\mu(x)\ , \tag{1}$$
$$I(A,j;T;-)=I^\dagger(A,j;T;+),\ \partial_\mu j^\mu(x)=0\ ,$$

where $A_\mu(x;+)$ and $A_\mu(x;-)=A_\mu^\dagger(x;+)$ are the positive- and negative-frequency free-photon four-potentials. The S matrix, suitable for describing the spontaneous emission in a dielectric medium, i.e., the multiphoton processes in which the electron recoil is neglected, is given as [3]

$$S(T)=\exp\left[-\frac{\langle m(T)\rangle}{2}\right]\exp[iI(A,j;T;-)]$$
$$\times\exp[iI(A,j;T;+)]\ . \tag{2}$$

Here $\langle m(T)\rangle$, the total number of photons of any polarization emitted spontaneously over interaction time T, is formally given as the commutator of action integrals [3], which, with the quantization rules for $A^\mu(x)$ [1], is evaluated to be [3]

$$\langle m(T)\rangle=[I(A,j;T;+),I(A,j;T;-)]$$
$$=i\int_{-T/2}^{T/2}dt_x\int_{-T/2}^{T/2}dt_y\int d^3x\,d^3y\,j^\mu(x)j^\nu(y)D_{\mu\nu}^{(+)}(x-y) \tag{3a}$$
$$=\frac{i}{(2\pi)^4}\int d^4k\,\tilde{j}^{\mu*}(k;T)D_{\mu\nu}^{(+)}(k)\tilde{j}^{\nu}(k;T)\ . \tag{3b}$$

Here $D_{\mu\nu}^{(+)}(k)$ is the four-dimensional Fourier transform of positive-frequency singular function $D_{\mu\nu}^{(+)}(x)$, which for a medium at rest becomes [1]

$$D_{\mu\nu}^{(+)}(k)\to D_{ij}^{(+)}(k)=-i\pi P_{ij}(\hat{\mathbf{k}})\frac{\theta(\omega)}{|\mathbf{k}|}\delta(|\mathbf{k}|-n\omega)\ , \tag{4a}$$
$$P_{ij}(\hat{\mathbf{k}})=\delta_{ij}-\hat{\mathbf{k}}_i\hat{\mathbf{k}}_i\ , \tag{4b}$$

where, appropriately, the fourth component of the four-momentum has been identified as photon's angular frequency ω, and

$$\tilde{j}^\mu(k;T)=\int_{-T/2}^{T/2}dt_x\int d^3x\,e^{-ikx}j^\mu(x)\ . \tag{5}$$

One should notice that the index of refraction n may depend on ω. As we see, through relations (3)–(5), the S matrix conveniently contains a simultaneous dependence on n, the index of refraction, and T, the finite, rather than infinite, interaction time. As compared to Ref. [2], where the S matrix is describing radiation in a medium over an infinite interaction time, this is an improvement. For now, the angular energy distributions, etc., will depend explicitly on finite interaction time T.

Now, in order to arrive at expressions for emission energy, power spectra, angular energy, and power distributions, we utilize $\langle m(T)\rangle$ from relations (3). By noticing that $d^3k=|\mathbf{k}|^2d|\mathbf{k}|d\Omega$, relation (3b) is rewritten as

$$\langle m(T)\rangle=\int\frac{d\omega\,d\Omega}{\omega}\left[\frac{d^2W(\omega;T)}{d\omega\,d\Omega}\right]\ , \tag{6a}$$
$$\frac{dW(\omega;T)}{d\omega}=\int d\Omega\left[\frac{d^2W(\omega;T)}{d\omega\,d\Omega}\right]\ , \tag{6b}$$
$$\frac{dP(\omega)}{d\Omega}=\frac{1}{T}\frac{d^2W(\omega;T)}{d\omega\,d\Omega}\ , \tag{6c}$$
$$P(\omega)=\frac{1}{T}\frac{dW(\omega;T)}{d\omega}\ , \tag{6d}$$

where $dW(\omega;T)/d\omega$, $d^2W(\omega;T)/d\omega d\Omega$, $P(\omega)$, and $dP(\omega)/d\Omega$ are the emission energy spectrum, angular-spectral energy distribution, power spectrum, and angular power spectrum distribution, respectively. From these definitions we also obtain that for spontaneously emitted radiation, the expressions for the angular energy distribution and the total energy are

$$\frac{dW(T)}{d\Omega}=\int d\omega\left[\frac{d^2W(\omega;T)}{d\omega\, d\Omega}\right], \tag{7a}$$

$$W(T)=\int d\Omega\left[\frac{dW(T)}{d\Omega}\right]. \tag{7b}$$

Now, for a medium at rest ($n\omega=|\mathbf{k}|$), we use relations (4) which, after having integrated the δ function, yield

$$\frac{d^2W(\omega;T)}{d\omega\, d\Omega}=\frac{n\omega^2}{16\pi^3}\rho^2(\hat{\mathbf{k}},\omega;T), \tag{8}$$

$$\rho^2(\hat{\mathbf{k}},\omega;T)=j_i^*(\hat{\mathbf{k}},\omega;T)P_{ij}(\hat{\mathbf{k}})j_j(\hat{\mathbf{k}},\omega;T), \tag{9a}$$

$$j_i(\hat{\mathbf{k}},\omega;T)\equiv\tilde{j}_i(\mathbf{k}=\hat{\mathbf{k}}n\omega,\omega;T), \tag{9b}$$

where one should keep in mind that n may depend on ω. From relation (8), with the help of relations (6) and (7), we obtain $\langle m(T)\rangle$, $dW/d\omega$, $dP/d\Omega$, $P(\omega)$, $dW/d\Omega$, and W.

III. SPONTANEOUS RADIATION IN A MEDIUM WITH A UNIFORM MAGNETIC FIELD; HELICAL ČERENKOV EFFECT

In this section we elaborate on spontaneous emission in a dielectric medium due to a uniform magnetic field. Particularly we shall be interested in deriving the helical Čerenkov effect and seeing under what conditions the spontaneous emission in a medium can go into the fundamental and the higher-harmonic frequencies.

Next, we choose the uniform magnetic field to be in the z direction, $\mathbf{B}=\hat{\mathbf{z}}B$, which causes an electron to spiral with the velocity and the position, respectively, as [3]

$$\mathbf{v}(t)=\mathbf{v}_\perp(t)+\hat{\mathbf{z}}v_3^0, \tag{10a}$$

$$\mathbf{v}_\perp(t)=v_\perp[-\hat{\mathbf{x}}\sin(\omega_c t+\alpha)+\hat{\mathbf{y}}\cos(\omega_c t+\alpha)]; \tag{10b}$$

$$\mathbf{r}(t)=\mathbf{r}_\perp(t)+\hat{\mathbf{z}}x_3(t), \tag{11a}$$

$$x_3(t)=v_3^0 t+x_3^0; \tag{11b}$$

$$\mathbf{r}_\perp(t)=(v_\perp/\omega_c)[\hat{\mathbf{x}}\cos(\omega_c t+\alpha)+\hat{\mathbf{y}}\sin(\omega_c t+\alpha)]+\mathbf{R}_\perp^0,$$
$$\mathbf{R}_\perp^0=\mathbf{r}_\perp^0+\mathbf{r}_\perp^0(B),\quad \mathbf{r}_\perp^0=\hat{\mathbf{x}}x_1^0+\hat{\mathbf{y}}x_2^0, \tag{11c}$$
$$\mathbf{r}_\perp^0(B)=(-v_\perp/\omega_c)[\hat{\mathbf{x}}\cos\alpha+\hat{\mathbf{y}}\sin\alpha].$$

Here, $t=x^4$, α is a constant phase (to be determined shortly), $v_\perp=|\mathbf{v}_\perp(t)|$ is a constant magnitude of the electron perpendicular velocity, and ω_c is the electron relativistic angular cyclotron frequency

$$\omega_c=eB/M\gamma, \tag{12}$$

with M being electron mass, $\gamma=(1-\mathbf{v}^2)^{-1/2}$, and we took e to be negative of the electron charge, $e>0$.

We wrote the solution for $\mathbf{r}(t)$ in such a way that in the absence of the uniform magnetic field, $B=0$ ($\omega_c=0$), we obtain

$$\mathbf{r}(t;B=0)=\mathbf{r}_\perp(t;B=0)+\hat{\mathbf{z}}x_3(t),$$
$$\mathbf{r}_\perp(t;B=0)=\mathbf{r}_\perp^0+\hat{\mathbf{x}}v_1^0 t+\hat{\mathbf{y}}v_2^0 t, \tag{13a}$$
$$v_1^0=-v_\perp\sin\alpha,\quad v_2^0=v_\perp\cos\alpha.$$

From here we see that α is determined from $\tan\alpha=-v_1^0/v_2^0$. We can further elucidate α by introducing

$$\mathbf{v}_0=v_0\hat{\mathbf{v}}_0,$$
$$\hat{\mathbf{v}}_0=\hat{\mathbf{x}}\sin\theta_0\cos\phi_0+\hat{\mathbf{y}}\sin\theta_0\sin\phi_0+\hat{\mathbf{z}}\cos\theta_0, \tag{13b}$$
$$v_\perp^0=v_\perp,$$

which, when compared to relations (10) at $\omega_c=0$, yield

$$\cos\theta_0=v_3^0/v_0,\quad \sin\theta_0=v_\perp^0/v_0,$$
$$\cos\phi_0=-\sin\alpha,\quad \sin\phi_0=\cos\alpha,\quad \phi_0=\alpha+\frac{\pi}{2}, \tag{13c}$$

so that

$$\hat{\mathbf{v}}_0=-\hat{\mathbf{x}}\frac{v_\perp}{v_0}\sin\alpha+\hat{\mathbf{y}}\frac{v_\perp}{v_0}\cos\alpha+\hat{\mathbf{z}}\left[1-\frac{v_\perp^2}{v_0^2}\right]^{1/2}. \tag{13d}$$

In general, the expression for the four-vector electron current density is

$$j^\mu(\mathbf{x},t_x)=-ev^\mu(t_x)\delta(\mathbf{x}-\mathbf{r}(t_x)),$$
$$v^\mu(t_x)=(\mathbf{v}(t_x),1), \tag{14a}$$

which we shall use. As indicated by (5), the finite interaction time T Fourier transform of $j^\mu(\mathbf{x},t_x)$ is

$$\tilde{j}^\mu(k;T)=-e\tilde{e}\int_{-T/2}^{T/2}dt_x v^\mu(t_x)\exp\{i[t_x(\omega-v_3^0|\mathbf{k}|\cos\theta)-\xi(|\mathbf{k}|)\cos(\omega_c t_x+\alpha-\phi)]\}\tilde{e}_c,$$

$$\tilde{e}=\exp[-i\mathbf{k}\cdot(\mathbf{r}_\perp^0+\hat{\mathbf{z}}x_3^0)],\quad \tilde{e}_c=\exp[i\xi(|\mathbf{k}|)\cos(\alpha-\phi)], \tag{14b}$$

$$\xi(|\mathbf{k}|)=\frac{|\mathbf{k}|v_\perp\sin\theta}{\omega_c},$$

where we used relations (10) and (11), and

$$\hat{\mathbf{k}}=\hat{\mathbf{x}}\sin\theta\cos\phi+\hat{\mathbf{y}}\sin\theta\sin\phi+\hat{\mathbf{z}}\cos\theta\ . \tag{15}$$

Phase factor $\tilde{e}_c$ assures that $\tilde{j}^{\mu}$ is associated with a free electron when $\omega_c\to 0$. Formally this phase factor can be dropped when calculating, say, energy spectra from relations (3)–(7). For a vacuum this is indeed the case since a free particle does not radiate. In a medium, however, a free charged particle radiates by means of a Čerenkov effect and, in order to avoid any ambiguity in the derivation of the helical Černekov effect, we shall keep phase factor $\tilde{e}_c$ in definition of the electron current density.

A. The usual Čerenkov effect

We first derive the usual Čerenkov effect, so that the helical Čerenkov effect, derived later, can be compared with it. Taking the $\omega_c\to 0$ limit in relation (14b) and taking into account (13) and (9b), we obtain

$$\begin{aligned}&\tilde{j}^{\mu}(\hat{\mathbf{k}},\omega;T)=-ev_0^{\mu}2\pi\tilde{e}\,\delta(\omega[1-n(\omega)v_0\cos\theta_c];T)\ ,\\ &v_0^{\mu}=(\mathbf{v}_0,1),\mathbf{k}=\hat{\mathbf{k}}n\omega\ ,\\ &\cos\theta_c=\hat{\mathbf{k}}\cdot\hat{\mathbf{v}}_0=\sin\theta\sin\theta_0\cos(\phi-\phi_0)+\cos\theta\cos\theta_0\ .\end{aligned} \tag{16}$$

Here the finite time δ function is given by

$$\delta(s;T)=\frac{1}{2\pi}\int_{-T/2}^{T/2}dt\,e^{ist}=\frac{\sin(sT/2)}{\pi s}\ , \tag{17a}$$

where $\delta(s;T)$ is significantly different from zero for

$$|s|\lesssim\frac{2\pi}{T}\ . \tag{17b}$$

Furthermore, we have

$$\delta(-s;T)=\delta(s;T)\ , \tag{18a}$$

$$\delta(0;T)=T/2\pi\ ; \tag{18b}$$

$$\delta(as;T)=\frac{1}{|a|}\delta(s;\tilde{T}),\tilde{T}=|a|T; \tag{18c}$$

$$\delta(s;T\to\infty)=\delta(s)\ , \tag{18d}$$

and for the sufficiently large T from (17b) and (18b) we deduce that $(n,m=0,\pm1,\pm2,\ldots)$

$$\delta(s_n;T)\delta(s_m;T)\cong\frac{T}{2\pi}\delta_{nm}\delta(s_n;T)\ , \tag{19}$$

where it is assumed that $s_n\neq s_m$ if $n\neq m$. As we see, for a sufficiently large T the finite time δ functions behave very much like ordinary δ functions.

Next, according to relations (8) and (9), we evaluate $\rho^2(\hat{\mathbf{k}},\omega;T)$ as

$$\begin{aligned}\rho^2(\hat{\mathbf{k}},\omega;T)=&16\pi^3\alpha v_0^2(1-\cos^2\theta_c)\\ &\times\delta^2(\omega[1-n(\omega)v_0\cos\theta_c];T)\ ,\end{aligned} \tag{20}$$

where $\alpha=e^2/4\pi$ and the definition of θ_c from relation (16) has been taken into account. Furthermore, with the help of (18b), (18c), and (19), for a sufficiently large T, say $T\gg 2\pi/\omega$, we can treat the finite time δ function as an ordinary δ function, giving

$$\begin{aligned}\rho^2(\hat{\mathbf{k}},\omega;T)\simeq&\frac{8\pi^2\alpha v_0T}{\omega n(\omega)}\left[1-\frac{1}{n^2(\omega)v_0^2}\right]\\ &\times\delta\left[\left[\cos\theta_c-\frac{1}{n(\omega)v_0}\right];\tilde{T}\right],\\ \tilde{T}=&T\omega v_0n(\omega),\quad\cos\theta_c\cong 1/n(\omega)v_0\ .\end{aligned} \tag{21}$$

According to relation (8), the angular-spectral energy distribution of the Čerenkov radiation is

$$\begin{aligned}\frac{d^2W(\omega;T)}{d\omega\,d\Omega_c}=&\frac{\alpha\omega v_0T}{2\pi}\left[1-\frac{1}{n^2(\omega)v_0^2}\right]\\ &\times\delta\left[\left[\cos\theta_c-\frac{1}{n(\omega)v_0}\right];\tilde{T}\right],\end{aligned} \tag{22}$$

where $d\Omega_C\equiv d\phi_C d\cos\theta_C$. Relation (22), with the help of relations (6b) and (6d) yields a familiar form for the expression of the power spectrum of the Čerenkov radiation [1]

$$P(\omega)\cong\alpha\omega v_0\left[1-\frac{1}{n^2(\omega)v_0^2}\right]\ . \tag{23}$$

B. The helical Čerenkov effect and the higher harmonic spontaneous emission

When the uniform magnetic field is different from zero ($B\neq 0,\omega_c\neq 0$), the expression for $\tilde{j}^{\mu}$ from (14b) can be integrated over t_x only if $\hat{\mathbf{k}}$ is collinear with **B**. To deal with the general case, we use

$$e^{-iz\cos\beta}=\sum_{l=-\infty}^{\infty}(-i)^lJ_l(z)e^{\pm il\beta}\ , \tag{24}$$

where J_l is the Bessel function. When applying relation (24) to the term in (14b) containing a cosine function and taking into account relations (9b) and (10b), we obtain $(n\omega=|\mathbf{k}|)$

$$j_1(\hat{\mathbf{k}},\omega;T)=-ie\tilde{e}\,\tilde{e}_c\pi v_{\perp}\sum_{l=-\infty}^{\infty}(-i)^{l+1}e^{-il\alpha}\delta(\omega(1-nv_3^0\cos\theta)-l\omega_c;T)\{e^{i(l+1)\phi}J_{l+1}(\xi)+e^{i(l-1)\phi}J_{l-1}(\xi)\}\ , \tag{25a}$$

$$j_2(\hat{\mathbf{k}},\omega;T)=-e\tilde{e}\tilde{e}_c\pi v_{\perp}\sum_{l=-\infty}^{\infty}(-i)^{l+1}e^{-il\alpha}\delta(\omega(1-nv_3^0\cos\theta)-l\omega_c;T)\{e^{i(l+1)\phi}J_{l+1}(\xi)-e^{i(l-1)\phi}J_{l-1}(\xi)\}\ , \tag{25b}$$

$$j_3(\hat{\mathbf{k}},\omega;T)=-2e\tilde{e}\tilde{e}_c\pi v_3^0\sum_{l=-\infty}^{\infty}(-i)^le^{il(\phi-\alpha)}\delta(\omega(1-nv_3^0\cos\theta)-l\omega_c;T)J_l(\xi)\ , \tag{25c}$$

$$j^4(\hat{\mathbf{k}},\omega;T)=j_3(\hat{\mathbf{k}},\omega;T)/v_3^0\ , \tag{25d}$$

where now

$$\xi=\frac{n(\omega)\omega v_\perp\sin\theta}{\omega_c} , \tag{25e}$$

and finite time δ function is given by relation (17). As we can see from relations (25), the expansions of the Fourier transforms of the current density components at the physical photon momentum ($n\omega=|\mathbf{k}|$) involves also $l\leq 0$, rather than just $l>0$, when $n(\omega)\neq 1$. For example, for sufficiently large T, if $1-n(\omega)v_3^0\cos\theta<0$, terms with $l<0$ will dominate in (25).

As they now stand, relations (25) are definitely correct. However, in maintaining a practical point of view, we shall assume that interaction time T is rather large, say $T\gg(2\pi/\omega_c)$. Now, as in the case of $n=1$ (a vacuum), we still may call l a harmonic index; however, since generally n may depend on ω, it may not always be a simple matter to determine how ω and l are related. Specifically we can define the radiation resonance angular frequencies from relations (25) as

$$\bar{\omega}(l)\{1-n(\bar{\omega}(l))v_3^0\cos\theta\}-l\omega_c=0 . \tag{26}$$

Relation (26) is simply the constraint on $\bar{\omega}(l)$, θ, and l; only two of them can be viewed as independent parameters. As we see, for fixed l and θ, it is not always a simple matter to determine $\bar{\omega}(l)$. As usual, the off-resonance angular frequency is defined by

$$\delta\omega_l=[1-v_3^0 n(\bar{\omega}(l))\cos\theta][\omega-\bar{\omega}(l)] . \tag{27}$$

As in the case of a vacuum, it is again a free parameter, telling us how the true ω differs from the $\bar{\omega}(l)$. However, for sufficiently large T, $T\gg 2\pi/\omega_c$, we have from (17b) that

$$|\omega[1-v_3^0 n(\omega)\cos\theta]-l\omega_c|\lesssim\frac{2\pi}{T}\ll\omega_c . \tag{28}$$

Comparison of (28) with (26) tells us that, from a practical point of view, in an expression that is dominated with a δ function containing a specific l, we need not distinguish between ω and $\bar{\omega}(l)$, as we can set $\omega=\bar{\omega}(l)$ everywhere except in the δ function itself [3].

At this point we introduce the photon orthonormal polarization unit vectors valid in any reference frame [3].

$$\begin{aligned}&\hat{\boldsymbol{\eta}}(\hat{\mathbf{k}},1)=\hat{\mathbf{x}}\cos\theta\cos\phi+\hat{\mathbf{y}}\cos\theta\sin\phi-\hat{\mathbf{z}}\sin\theta ,\\ &\hat{\boldsymbol{\eta}}(\hat{\mathbf{k}},2)=-\hat{\mathbf{x}}\sin\phi+\hat{\mathbf{y}}\cos\phi,\quad \hat{\boldsymbol{\eta}}(\hat{\mathbf{k}},3)=\hat{\mathbf{k}} ,\end{aligned} \tag{29}$$

where $\hat{\mathbf{k}}$ is given by (15). In terms of these vectors, the photon circular polarization unit vectors are [3] ($\beta=\pm1$):

$$\begin{aligned}\hat{\boldsymbol{\epsilon}}(\hat{\mathbf{k}},\beta)&=\frac{1}{\sqrt{2}}[\hat{\boldsymbol{\eta}}(\hat{\mathbf{k}},1)+i\beta\hat{\boldsymbol{\eta}}(\hat{\mathbf{k}},2)]\\ &=\frac{\exp(-i\beta\phi)}{2}(\cos\theta+1)\hat{\boldsymbol{\epsilon}}_0(\beta)\\ &\quad+\frac{\exp(i\beta\phi)}{2}(\cos\theta-1)\hat{\boldsymbol{\epsilon}}_0(-\beta)-\frac{\sin\theta}{\sqrt{z}}\hat{\mathbf{z}} ,\end{aligned} \tag{30a}$$

$$\hat{\boldsymbol{\epsilon}}_0(\beta)=\frac{1}{\sqrt{2}}(\hat{\mathbf{x}}+i\beta\hat{\mathbf{y}}) , \tag{30b}$$

$$\overset{*}{\hat{\boldsymbol{\epsilon}}}(\hat{\mathbf{k}},\beta)\cdot\hat{\boldsymbol{\epsilon}}(\hat{\mathbf{k}},\delta)=\delta_{\beta\delta} , \tag{30c}$$

$$\sum_{\beta=-1}^{1}\overset{*}{\hat{\boldsymbol{\epsilon}}}(\hat{\mathbf{k}},\beta)_i\hat{\boldsymbol{\epsilon}}(\hat{\mathbf{k}},\beta)_j=P_{ij}(\hat{\mathbf{k}}) , \tag{30d}$$

where P_{ij} is given by (4b). As in the case of a vacuum, we define

$$\begin{aligned}j_0(\hat{\mathbf{k}},\omega;\beta;T)&=\hat{\boldsymbol{\epsilon}}_0(\hat{\mathbf{k}},\beta)\cdot\mathbf{j}(\hat{\mathbf{k}},\omega;T)\\ &=-\sqrt{2}e\tilde{e}v_\perp\pi\sum_{l=-\infty}^{\infty}(-i)^l e^{-il\alpha}\delta(\omega[1-v_3^0 n(\omega)\cos\theta]-l\omega_c;T)e^{i(l+\beta)\phi}J_{l+\beta}(\xi) ,\end{aligned} \tag{31a}$$

where we took into account that

$$1\pm\beta=2\delta_{\beta(\pm1)},\quad \beta=\pm1 . \tag{31b}$$

With this, we finally have ($\beta=\pm1$)

$$\begin{aligned}j(\hat{\mathbf{k}},\omega;\beta;T)&=\hat{\boldsymbol{\epsilon}}(\hat{\mathbf{k}},\beta)\cdot\mathbf{j}(\hat{\mathbf{k}},\omega;T)\\ &=\frac{\exp(-i\beta\phi)}{2}(\cos\theta+1)j_0(\hat{\mathbf{k}},\omega;\beta;T)+\frac{\exp(i\beta\phi)}{2}(\cos\theta-1)j_0(\hat{\mathbf{k}},\omega;-\beta;T)-\frac{\sin\theta}{\sqrt{2}}j_3(\hat{\mathbf{k}},\omega;T)\end{aligned} \tag{32a}$$

$$\begin{aligned}&=-\frac{e\tilde{e}\pi}{\sqrt{2}}\sum_{l=-\infty}^{\infty}(-i)^l e^{il(\phi-\alpha)}\delta(\omega[1-n(\omega)v_3^0\cos\theta]-l\omega_c;T)\\ &\quad\times\{v_\perp[(\cos\theta+1)J_{l+\beta}(\xi)+(\cos\theta-1)J_{l-\beta}(\xi)]-2v_3^0\sin\theta J_l(\xi)\} .\end{aligned} \tag{32b}$$

With the help of relations (19), (18c), and (30d), relations (8), (9), and (32b) yield for the angular-spectral energy distribution

$$\frac{d^2W(\omega;T)}{d\omega d\Omega}=\sum_{l=-\infty}^{\infty}\frac{d^2W(\omega;T;l)}{d\omega d\Omega} , \tag{33a}$$

with the harmonic angular-spectral energy distribution given as

$$\frac{d^2W(\omega;T;l)}{d\omega\,d\Omega}=\frac{\alpha L\bar{\omega}(l)}{16\pi(v_3^0)^2}\sum_{\beta=-1}^{1}\delta\left[\cos\theta-\frac{l}{n(\omega)v_3^0}+\frac{l\omega_c}{n(\omega)v_3^0\omega};\tilde{T}\right]$$
$$\times\{v_\perp[(\cos\theta+1)J_{l+\beta}(\xi_l)+(\cos\theta-1)J_{l-\beta}(\xi_l)]-2v_3^0\sin\theta J_l(\xi_l)\}^2\,,$$
$$\tilde{T}=n(\omega)\omega v_3^0 T\,,$$
$$\xi_l=\frac{n(\bar{\omega}(l))\bar{\omega}(l)v_\perp\sin\theta}{\omega_c}\equiv\frac{n(\omega)\omega v_\perp}{\omega_c}\left[1-n_{(l)}^2\right]^{1/2}\,,$$
$$\cos\theta\cong\eta(l)=\frac{1}{n(\omega)v_3^0}\left[1-\frac{l\omega_c}{\omega}\right]<1\,. \tag{33b}$$

Here $L=v_3^0T$ is the interaction length, and, consistent with (26) and (28), we identified $\bar{\omega}(l)$ with ω. Let us point out that as long as relation (28) holds and once l is fixed, ω and θ are not completely independent from each other. This means that for a given θ, different ω's generally will appear at different l's. Conversely, for a given ω, different θ's generally will appear at different l's.

It is the presence of index of refraction $n(\omega)$ that requires nontrivial constraints involving θ, ω, and l. Namely, from relations (26) and (28) [$\bar{\omega}(l)\simeq\omega$], we have

$$\frac{l\omega_c}{\omega}\cong 1-n(\omega)v_3^0\cos\theta\,, \tag{34a}$$

implying

$$\mathrm{sgn}l\cong\mathrm{sgn}[1-n(\omega)v_3^0\cos\theta],\quad l\neq 0 \tag{34b}$$

$$n(\omega)v_3^0\cos\theta\cong 1,\quad l=0\,. \tag{34c}$$

Relation (34c) is nothing but the kinematics of the helical Čerenkov effect to be discussed shortly. From relations (34) we see that the spontaneous emission can occur in the vacuum, forward, and backward Čerenkov branches [1,2] with the corresponding l: For the vacuum branch,

$$n(\omega)v_3^0<1,\quad n(\omega)v_3^0\cos\theta<1,\quad l\geq 1\,; \tag{35a}$$

for the backward branch,

$$n(\omega)v_3^0>1,\quad n(\omega)v_3^0\cos\theta<1,\quad l\geq 1\,; \tag{35b}$$

and for the forward branch,

$$n(\omega)v_3^0\geq 1,\quad n(\omega)v_3^0\cos\theta\geq 1,\quad l\leq 0\,. \tag{35c}$$

The expression for angular-spectral energy distribution (33a) holds regardless of whether T, the interaction time, is large or small. However, with the assumption that T is large [$\bar{\omega}(l)\cong\omega$] we can treat the δ function in (33b) as an ordinary δ function yielding from (6b) the energy spectrum

$$\frac{dW(\omega;T)}{d\omega}=\sum_{l=-\infty}^{\infty}\frac{dW(\omega;T;l)}{d\omega}\,, \tag{36a}$$

with the harmonic energy spectrum as

$$\frac{dW(\omega;T;l)}{d\omega}=\frac{\alpha L}{8(v_3^0)^2}\sum_{\beta=-1}^{1}\omega\{v_\perp\{[1+\eta(\omega,l)]J_{l+\beta}[\xi(\omega,l)]$$
$$+[\eta(\omega,l)-1]J_{l-\beta}[\xi(\omega,l)]\}$$
$$-2v_3^0[1-\eta^2(\omega,l)]^{1/2}J_l[\xi(\omega,l)]\}^2\,,$$
$$\eta(\omega,l)\equiv\frac{1}{n(\omega)v_3^0}\left[1-\frac{l\omega_c}{\omega}\right]<1\,,$$
$$\xi(\omega;l)=\frac{n(\omega)\omega v_\perp[1-\eta^2(\omega,l)]^{1/2}}{\omega_c}\,. \tag{36b}$$

Numerically, of course $\eta(\omega,l)\cong\cos\theta$, except that now it is expressed in terms of ω. The angular power spectrum distribution and the power spectrum can be obtained by dividing relations (33) and (36) by T, respectively. Specifically for the power spectrum we have

$$P(\omega)=\sum_{l=-\infty}^{\infty}P(\omega;l)\,, \tag{37a}$$

$$P(\omega;l)=\frac{1}{T}\frac{dW(\omega;T;l)}{d\omega}\,. \tag{37b}$$

As for the evaluations of the angular energy distribution and the total energy, these can be done only after n is specified as a function of ω.

Now we can discuss the helical Čerenkov effect, which corresponds to the $l=0$ terms in relations (33)–(37). Taking into account that

$$J_{-n}(x)=J_n(-x)=(-1)^nJ_n(x)\,,$$

from relations (33b) we obtain that the angular-spectral energy distribution for the helical Čerenkov effect is

$$\frac{d^2W(\omega;T;0)}{d\omega\,d\Omega}=\frac{\alpha L\omega}{2\pi}\delta\left[\cos\theta_h-\frac{1}{n(\omega)v_3^0};\tilde{T}\right]\left\{(\sin^2\theta_h)J_0^2(\xi_0)+\left[\frac{v_\perp}{v_3^0}\right]^2J_1^2(\xi_0)\right\} \tag{38a}$$

$$\cong \frac{\alpha L\omega}{2\pi}\delta\left[\cos\theta_h - \frac{1}{n(\omega)v_3^0};\tilde{T}\right]\left\{\left[1-\frac{1}{[n(\omega)v_3^0]^2}\right]J_0^2(\xi_0)+\left[\frac{v_\perp}{v_3^0}\right]^2 J_1^2(\xi_0)\right\}, \tag{38b}$$

where $\theta=\theta_h$ denotes the radiation angle of the helical Čerenkov effect satisfying

$$\cos\theta_h = 1/n(\omega)v_3^0 , \tag{38c}$$

$$\xi_0 = \frac{n(\omega)\omega v_\perp \sin\theta_h}{\omega_c} ; \tag{38d}$$

that is, in going from (38a) to (38b), we assumed that T is sufficiently large so that we can treat the finite time δ function as an ordinary δ function. Integrating (38b) over the solid angle and dividing the result by T, or by dividing (38b) at $l=0$ by T, we obtain the power spectrum of the helical Čerenkov radiation to be

$$P(\omega;0)\cong\alpha\omega v_3^0\left\{\left[1-\frac{1}{[n(\omega)v_3^0]^2}\right]J_0^2(\xi_0) + \left[\frac{v_\perp}{v_3^0}\right]^2 J_1^2(\xi_0)\right\} . \tag{39}$$

Comparing the power spectra of the helical Čerenkov effect and the ordinary Čerenkov effect (23), we see that the former goes into the latter when $v_\perp\to 0$, since $J_n(\xi_0\to 0)\to\delta_{n0}$, as $\xi_0\to 0$. This is not surprising since when $v_\perp=0$ and $\mathbf{v}\times\mathbf{B}=\mathbf{0}$, the electron behaves as a free electron; that is, it does not feel the presence of the magnetic field.

To the total power spectrum in relations (37) we shall have contributions also from $l=\pm1,\pm2,\ldots$. Will these additional terms obscure the helical Čerenkov effect? Generally, no. The reason for this is that different l's have different kinematics. Namely, at the angle θ_h let the helical Čerenkov effect ($l=0$) occur with particular angular frequency ω. Then, as relation (34a) indicates, for the same $\theta=\theta_h$ but $l\neq 0$, we shall generally have different ω's. However, how do we find θ_h at which ($l=0$) helical Čerenkov effect occurs? This is simple, at least in principle. Namely, kinematics of the ordinary and helical Čerenkov effect are the same except that in the ordinary one v_0 comes, while in the helical one v_3^0 comes. Thus if we have that

$$v_3^0\ [\text{from Eq. (38c)}] = v_0\ [\text{from Eq. (21)}] , \tag{40a}$$

then we must have $n(\omega)\cos\theta_c$ [from Eq. (21)] $=n(\omega)\cos\theta_h$ [from Eq. (38c)]. As long as the dielectric is the same in both cases, one excepts ω to be the same also; hence, numerically we expect

$$\theta_h=\theta_c . \tag{40b}$$

In other words, if for a given dielectric we tabulate v_0 vs θ_c for the ordinary Čerenkov effect, relations (40a) and (40b) should tell us at which θ_h, for a given v_3^0, we should observe the helical Čerenkov effect. From relation (40a) it is clear that we need a larger electron velocity in the helical Čerenkov effect than in the ordinary Čerenkov effect if we are to observe the same radiation frequencies at the same angles.

In fact, from the preceding discussion we see the main characteristics that distinguish the helical Čerenkov effect from the ordinary Čerenkov effect: while the ordinary Černekov radiation travels down the cone of angle θ_c with respect to $\mathbf{v}_0$, the helical Čerenkov radiation travels down the cone of angle θ_h with respect to $\hat{\mathbf{B}}$. As a consequence, on the global level one should be able to detect in principle how the ordinary Čerenkov effect changes into the helical Čerenkov effect when a sufficiently strong uniform magnetic field is introduced into the dielectric: the Čerenkov radiation cone, whose axis is given by $\mathbf{v}_0$, changes into the helical Čerenkov radiation cone, whose axis is given by $\mathbf{B}$.

Next, let us deduce some geometric characteristics of the helical Čerenkov effect which are not present in the usual Čerenkov effect. Specifically, what we wish to show is that the helical Čerenkov effect, besides having a radiation cone whose axis is given by $\hat{\mathbf{B}}$, has a power spectrum that is quite different from the power spectrum of the ordinary Čerenkov effect. For example, it can be dominated by either J_0^2 or J_1^2 if the radius of curvature of the electron trajectory (measured in the plane perpendicular to the direction of the electron guiding center) is given in respective multiples of the radiation wavelength. To elaborate on the last point, let us assume that the electron guiding center is pointed in the z direction. Then the radius of curvature, as measured in the x-y plane [the electron trajectory in this plane is described by $x=x(t)$ and $y=y(t)$], is given by the expression

$$R(t)=\frac{(\dot{x}^2+\dot{y}^2)^{3/2}}{|\dot{x}\ddot{y}-\dot{y}\ddot{x}|} . \tag{41}$$

For the electron in a uniform magnetic field whose guiding center is in the $\hat{\mathbf{z}}=\hat{\mathbf{B}}$ direction, the application of relation to (41) to expression (11c) for $\mathbf{r}_\perp(t)$ yields

$$R=\frac{v_\perp}{\omega_c}=\frac{M\gamma v_\perp}{eB} , \tag{42}$$

which, when inserted into relation (38d), yields (with λ the radiation wavelength)

$$R=\frac{\lambda\xi_0}{2\pi n(\omega)\sin\theta_h} , \qquad \sin\theta_h=\left[1-\frac{1}{[n(\omega)v_3^0]^2}\right]^{1/2} . \tag{43}$$

Now, as demonstrated in Fig. 1, for $\xi_0\leq 2$, $J_0^2(\xi_0)$, and $J_1^2(\xi_0)$ have, respectively, single maxima, say $s=0$ maxima, at

$$\xi_{0M}(l=0,s=0)=0, \quad \xi_{0M}(l=1,s=0)=1.8 , \tag{44a}$$

while, in general for $\xi_0>2$, $J_l^2(\xi_0)$ have ($s=1,2,\ldots$)

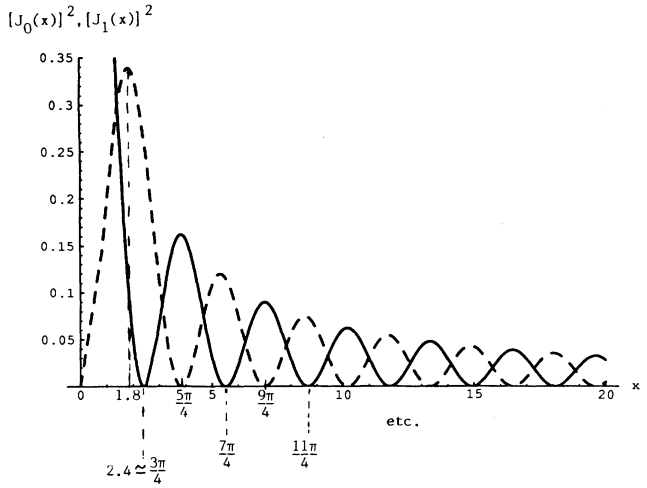

FIG. 1. The approximate positions of maxima and minima of both J_0^2 (solid line) and J_1^2 (dashed line) which are helpful in determining the helical Čerenkov effect power spectrum.

minima (zeros) and maxima approximately at, respectively,

$$\xi_{0m}(l,s)=(2l+4s-1)\left[\frac{\pi}{4}\right], \quad l=0,1,2,\ldots,s=1,2,3,\ldots, \tag{44b}$$

$$\xi_{0M}(l,s)=(2l+4s+1)\left[\frac{\pi}{4}\right], \quad l=0,1,2,\ldots,s=1,2,3,\ldots. \tag{44c}$$

Since for $\xi_0>2$ ($l=0,1,2,\ldots$, $s=1,2,\ldots$)

$$\xi_{0m}(l+1,s)=\xi_{0m}(l-1,s+1)=\xi_{0M}(l,s), \tag{45a}$$

we have that

$$\xi_{0m}(1,s)=\xi_{0M}(0,s), \quad \xi_{0m}(0,s+1)=\xi_{0M}(1,s). \tag{45b}$$

Relation (45b) and Fig. 1 show that for $\xi_0>(3\pi/4)\cong 2.4$, the positions of maxima (minima) of J_0^2 coincide with the positions of minima(maxima) of J_1^2; specifically at $\xi_0=5\pi/4, 9\pi/4, \ldots, J_0^2$ has maxima while $J_1^2\cong 0$, and at $\xi_0=7\pi/4, 11\pi/4, \ldots, J_1^2$ has maxima while $J_0^2\cong 0$. This means that as ξ_0 is varied from zero to larger values, the power spectrum of the helical Čerenkov effect is alternatively dominated by $(\sin\theta_h J_0)^2$ term ($J_1^2\cong 0$) or by J_1^2 term ($J_0^2\cong 0$), when we say that we have the "pure" helical Čerenkov effect power spectrum. We can enlighten this point by associating the minima and maxima of J_0^2 and J_1^2 with the radia of curvature of the electron trajectory. Substituting relations (44) into (43a), we obtain the corresponding curvature radia as

$$R_M(l=0,s=0)=0, \tag{46a}$$

$$R_M(l=1,s=0)=\frac{1.8\lambda}{2\pi n(\omega)\sin\theta_h}, \tag{46b}$$

$$R_m(l=0,s)=\frac{(4s-1)\lambda}{8n(\omega)\sin\theta_h}, \tag{47a}$$

$$R_m(l=1,s)=\frac{(4s+1)\lambda}{8n(\omega)\sin\theta_h}, \tag{47b}$$

$$R_M(l=0,s)=\frac{(4s+1)\lambda}{8n(\omega)\sin\theta_h}, \tag{48a}$$

$$R_M(l=1,s)=\frac{(4s+3)\lambda}{8n(\omega)\sin\theta_k}, \tag{48b}$$

where $s=1,2,\ldots$.

We see that at $\xi_0=0$, which is achieved by either $v_\perp=0$, $\omega_c\neq 0$, or $v_\perp\neq 0$, $\omega_c\to\infty$ ($B\to\infty$), $R=0$. As seen from (46a) now $J_0^2=1$, $J_l=0$, $l\neq 0$, and the power spectrum becomes qualitatively similar to the power spectrum of the ordinary Čerenkov effect. This shows that the power spectrum of the helical Čerenkov effect will assume more of the shape of the power spectrum of the ordinary Čerenkov effect (be more dominated by J_0^2) as the radius of curvature of the electron trajectory satisfies $R\ll\lambda$. Practically this could be achieved by increasing B and/or by decreasing $v_\perp$.

At this point we need to find out more specifically under which conditions it should be possible to observe experimentally the helical Čerenkov effect. Namely, following Fermi [7] Huybrecht and Schoenberg [8] have found that the total energy loss of an electron passing through a medium is distributed between ionization excitation and the Črenekov radiation. The contribution of the Čerenkov radiation to the total energy losses are generally quite significant [9]. In fact, the increase in losses beyond the minimum of the ionization curve for electrons with $\gamma\geq 4$ generally is determined completely by the Čerenkov radiation [9], particularly for lower frequency radiation [8,9] such as visible frequencies and smaller [10] (other relevant references on this subject can be found in Ref. [9]). We shall assume that the same things hold also for the helical Čerenkov effect and restrict our discussions about its experimental observability to radiation frequencies in the visible and below, and for fairly energetic electrons with kinetic energies of 1.5 MeV and above.

Next we notice that J_1^2 has the largest maximum at $\xi_0\cong 1.8$ (compare with Fig. 1). Now the radius of curvature of the electron trajectory is given by (46b) and for kinetic electron beam energies of 1.5 MeV and above, the helical Čerenkov radiation angle θ_h is not too far from $\theta_h^{\max}=\cos(1/n)$. Then, with $n(\omega)>1$, $n(\omega)\sin\theta_h\cong 1$, the dominance of term J_1^2 is going to be largest when, as relation (46b) suggests, $R\cong O(\lambda)$. Specifically for water as a medium with $n=1.33$ in the visible spectrum, $\lambda=(4$ to $7)\times 10^{-5}$ cm [10], with $\gamma_3=4$ ($v_3^0=0.968$), where

$$\gamma_3^2=\frac{1}{1-(v_3^0)^2}, \tag{49}$$

we definitively have $nv_3^0>1$. Relation (43b) gives $\sin\theta_h=0.63$ ($\theta_h\cong 39°$), which in turn, according to (46b), gives $R\cong 0.34\lambda$. Hence we may say that the helical Čerenkov effect will start superseding the ordinary Čerenkov effect (that is, J_1^2 will start to dominate in the

spectrum), at least for medium to high-energy electrons when the radius of curvature of the electron trajectory starts satisfying $R \cong O(\lambda)$.

We can estimate what strength of uniform magnetic field is needed to have $R \cong (\lambda)$ for different regions of the electromagnetic spectrum. From relation (42) we have

$$B=\frac{\gamma v_\perp}{R(e/M)}, \quad \gamma=\frac{\gamma_3}{[1-(\gamma_3 v_\perp)^2]^{1/2}}, \tag{50}$$

where $e/M \cong 1.8\times 10^{11}$ $s^{-1}T^{-1}$. Choosing $v_\perp = 2\times 10^{-3}$, $\lambda \cong 7\times 10^{-5}$ cm, and other parameters as given after relation (49), we obtain $B \cong 47$ T, which is a rather large field. Suppose that we can achieve experimentally $v_\perp \cong 2\times 10^{-4}$; then B would drop down to 4.7 T. However, because $(v_\perp/v_3^0)^2$ multiplies J_1^2 in the power spectrum despite the fact that J_1^2 is at its maximum, the term $(\sin\theta_h J_0)^2 \cong 0.005$ clearly dominates the power spectrum of the helical Čerenkov effect. However, if we choose $\lambda \cong 10^{-1}$ cm, $v_3^0 \cong 0.9$, $v_\perp \cong 0.4$ ($\gamma \cong 6$), and assuming a medium with $n \cong 1.4$, then at $R \cong \lambda$ we obtain $B \cong 4$ T, which is achievable. Furthermore, now $(v_\perp/v_3^0)^2 \cong 0.2$, allowing J_1^2 to dominate the power spectrum. In other words, in the microwave region one should be able to achieve the dominance of the pure helical Čerenkov term in the power spectrum when the beam is rather energetic.

As we formally increase ξ_0 beyond 2.4 the power spectrum of the helical Čerenkov effect will be completely dominated by either J_0^2 (when $J_1^2=0$) or by J_1^2 (when $J_0^2=0$) at $\xi_0=(4s+1)(\pi/4)$ and $\xi_0=(4s+3)(\pi/4)$, respectively [$s=1,2,\ldots$; compare with relations (44)]. Now taking that at $\gamma_3 \cong 3$ and $n=1.5$ typically [12] we have $\sin\theta_h \cong 0.7$, relations (48) tell us that approximately $R_M(l=0,1) \cong 5\lambda$ at $s=10$. At such a radius of curvature we have [compare with relations (44)] $J_0^2(41\pi/4) \cong J_1^2(43\pi/4) \cong 0.02$, $J_0^2(43\pi/4) \cong J_1^2(41\pi/4) \cong 0$. These values give finite measurable power spectra. However, since now R is so much larger, at $\lambda \cong 10^{-1}$ cm and for $v_\perp \cong 0.2$ ($\gamma \cong 4$), we need only $B \cong 0.4$ T. It is evident, however, that for $R \gg \lambda$, the helical Čerenkov effect becomes very weak, since $J_l^2(x)$ tends to zero at $x \to \infty$.

For the sake of completeness we write down the magnetic-field values at which the pure helical Čerenkov effect occurs. Namely the pure helical Čerenkov effect occurs when $J_0^2=0$ and J_1^2 is at its maxima, which after substituting (48b) into (50) yields for the magnetic field values

$$B_M(l=1,s)=\frac{8\gamma v_\perp n(\omega)\sin\theta_h}{(e/M)(4s+3)\lambda}, \quad s=1,2,\ldots. \tag{51}$$

As we see, sufficiently large s should yield a manageable B.

In general, the electron may have a rather complicated trajectory. Let us assume that it can be broken into a large number of segments each representing an ordinary helical trajectory. If the length of segment s is ΔL, and it takes electron Δt time to pass it, then the velocity of the electron guiding center in this segment is $v_g(s)=\Delta L/\Delta t$. Of course, each segment has its own radius of curvature, measured perpendicular to the direction of the guiding center, in term of which ξ_0 is now given as

$$\xi_0(s)=\frac{R(s)\omega}{v_g(s)}\{[n(\omega)v_g(s)]^2-1\}^{1/2}. \tag{52}$$

The power spectrum for segment s of the electron trajectory is given by relation (39) in which v_3^0 is replaced by $v_g(s)$ and $v_\perp$ by $v_\perp(s), v_\perp(s)$ being the magnitude of the perpendicular component of the electron velocity with respect to the direction of $v_g(s)$. As we see it, the helical Čerenkov effect is not restricted to just simple helical trajectories.

Finally we discuss the spontaneous emission with $l \neq 0$ in the situation when the index of refraction is a slowly varying function of the radiation frequency in some range of frequencies, all of which are assumed to be much smaller than some resonance frequency. According to relation (34a), for each $l \neq 0$, there corresponds a radiation angular frequency [compare with relations (34)]

$$\omega_l \cong \frac{|l|\omega_c}{|1-nv_3^0\cos\theta|}, \quad l=\pm 1,\pm 2,\ldots, \tag{53}$$

which is valid for either the vacuum or Čerenkov branch. Again ω_0, which corresponds to the helical Čerenkov effect, $1-nv_3^0\cos\theta_0=0$, should be determined as already outlined in relations (40). Furthermore we have a very important fact: the angle θ_h from the helical Čerenkov radiation is different from the angle (or angles) at which the spontaneous radiations with ω_l ($\omega \neq 0$) occurs. This fact follows simply from the inequality

$$\cos\theta_h=\frac{1}{nv_3^0} \neq \cos\theta=\frac{1}{nv_3^0}-\frac{l\omega_c}{nv_3^0\omega_l}, \quad l\neq 0,$$

which follows from relations (38c) and (34a) and which is exact since n is assumed to be independent of ω. Consequently, in the angular-spectral and angular-energy distributions for spontaneous emission for ω_l from (53), the helical Čerenkov effect can be ignored. Next, keeping in mind that T is assumed to be large, relation (28), we obtain from relation (33) the angular energy distribution to be

$$\frac{dW(\theta;T)}{d\cos\theta} \equiv w(\theta;T)=\sum_{(l\neq 0)}\frac{dW(\theta;T;l)}{d\cos\theta},$$

$$\frac{dW(\theta;T;l)}{d\cos\theta} \equiv w(\theta;T;l) \cong \frac{\alpha L l^2 n\omega_c^2}{8v_3^0|1-nv_3^0\cos\theta|^3}\sum_{\beta=-1}^{1}\{v_\perp[(\cos\theta+1)J_{l+\beta}(\xi_l)+(\cos\theta-1)J_{l-\beta}(\xi_l)]-2v_3^0\sin\theta J_l(\xi_l)\}^2, \tag{54a}$$

$$\xi_l=\left|\frac{l}{1-nv_3^0\cos\theta}\right| nv_\perp\sin\theta, \quad \xi_{-l}=\xi_l, \tag{54b}$$

where formally $w(\theta;T;l)$ is the angular energy distribution associated with the fundamental or harmonic frequency $f_l=\omega_l/2\pi$. Of course, for fixed θ for each $l\neq 0$ there corresponds ω_l, as determined by (53).

Now, we discuss numerically relations (54), that is, the angular energy distribution of spontaneously emitted radiation when n is practical constant in the radiation frequency over the spectral region of interest. When radiation angle θ is fixed, $1-nv_3^0\cos\theta$ is positive (negative) so that [compare with (34b) and (53)] $l=+1(-1)$ represents the fundamental radiation frequency and $l=+2\,(-2),\ +3(-3),\ldots,$ represent the harmonic frequencies. Clearly, $dW(\theta;T;l)$ measures how much of the spontaneously emitted energy over interaction length L with the frequency f_l goes into solid angle $2\pi\sin\theta\,d\theta$.

Specifically we choose $B=4$ T, $L=100$ cm, $v_3^0=0.63$, $v_\perp=0.6\{v=[(v_3^0)^2+v_\perp^2]^{1/2}=0.87,\gamma=2.03\}$. For $n=1.4$ we are in the vacuum branch and only positive l's come for any θ. For $\theta=0$ rad only $l=1$ can come and relations (53) and (54) yield $w=w(1)=0.61$ eV, $f_1=5.3\times10^{11}$ Hz. However, for $\theta=0.1$ rad with other parameters the same, we obtain many more contributions which are exhibited in Table I. Neglecting $w(l\geq 38)$, the sum over the fundamental and harmonic frequencies from Table I yields for the angular distribution the value $w(\theta=0.1\text{ rad})\cong 4.16$ eV. However, if the spontaneous emission is occurring in vacuum, $n=1$, rather than in the $n=1.4$ dielectric medium, the sum over the fundamental and harmonic frequencies would yield for the angular energy distribution only $w(\theta=0.1\text{ rad})\cong 0.03$ eV. As we see, the presence of the dielectric medium increased the spontaneous emission into solid angle $2\pi\sin\theta\,d\theta$ (at $\theta=0.1$ rad) by more than 138 times.

Now we choose $n=1.65, v_3^0=0.7, v_\perp=0.6$ $(v=0.92,\gamma\cong 2.6)$, so that the spontaneous emission will occur in the Čerenkov branch; with $\theta=0.1$ rad, it will occur in the backward Čerenkov branch since $\theta>\theta_h$. The contribution to the angular energy distribution comes only from $l<0$. Since $J_{-n}=(-1)_n J_n$ and $(-1)_\beta=(-1)$ for $\beta=\pm1$, the angular energy distributions are calculated by substituting $l\rightarrow|l|$ and changing the sign in the last term in relation (54b), $J_l\rightarrow -J_l$. With $B=4$ T and $L=100$ cm, at $\theta=0.1$ rad, the angular energy distributions are listed in Table II. Neglecting $w(l\leq -32)$, the sum over the fundamental and harmonic frequencies from Table II yields for the angular energy distribution the value $w(\theta=0.1\text{ rad})\cong 1.5$ eV, which is of the same order of magnitude as the example from the vacuum branch.

TABLE I. Vacuum branch angular energy distributions from relation (54b) for $B=4$ T, $L=100$ cm, $v_3^0=0.63$, $v_\perp=0.6$, $n=1.4$, and $\theta=0.1$ rad.

l	f_l (Hz)	$w(l)$ (eV)
1	5.13×10^{11}	0.39
2	1.02×10^{12}	0.58
3	1.54×10^{12}	0.60
4	2.05×10^{12}	0.55
5	2.56×10^{12}	0.45
10	5.13×10^{12}	0.13
25	1.28×10^{13}	9.14×10^{-4}
37	1.90×10^{13}	1.34×10^{-5}
≥ 38	$\sim10^{-6}$	

TABLE II. Backward Čerenkov branch angular energy distributions from relation (54b) for $B=4$ T, $L=100$ cm, $v_3^0=0.7$, $v_\perp=0.6, n=1.65$, and $\theta=0.1$ rad.

l	f_l (Hz)	$w(l)$ (eV)
-1	3.3×10^{11}	0.17
-2	6.61×10^{11}	0.24
-3	9.92×10^{11}	0.24
-4	1.32×10^{12}	0.21
-5	1.66×10^{12}	0.17
-10	3.31×10^{12}	3.73×10^{-2}
-20	6.61×10^{12}	8.92×10^{-4}
-31	1.02×10^{13}	1.05×10^{-5}
≤ -32		$\sim10^{-6}$

IV. DISCUSSION AND CONCLUSION

The first thing to notice is that, like the ordinary Čerenkov effect, the helical Čerenkov effect is a classical effect in the sense that Planck constant h does not appear in its power spectrum. The classical nature of the helical Čerenkov effect is directly evident from out derivation. Namely, when the electron recoil can be neglected, the electron current density is a classical quantity and the process involves only soft photons. The total energy carried by a moderate number of photons is negligible as compared to the energy of the electron. In such circumstances the quantum theory gives simply the statistical fluctuations around the results of classical electrodynamics [3]. The ordinary Čerenkov effect can be viewed as the electromagnetic shock radiation caused by a free electron with the velocity exceeding the velocity of the radiation in the medium [10]. The helical Čerenkov effect can also be viewed as the electromagnetic shock radiation, however, caused by an electron moving on a helical orbit with the velocity of its guiding center exceeding the velocity of the radiation in the medium.

There is no doubt that the presence of the dielectric medium enhances significantly the efficiency of the spontaneous electron radiation into the fundamental and harmonic frequencies ($l\neq 0$), as demonstrated by relations (55) and (56). Furthermore, let us mention that the helical Čerenkov effect, rather than the usually Čerenkov effect, should be used to answer the question as to how the electron beam when guided by the uniform magnetic field radiates when passing very close to the dielectric, such as quartz [2].

Finally, let us compare our work on spontaneous emission in a uniform magnetic field with a dielectric medium with works by Schwinger, Tsai, and Erber [11] and by Kroll [12], who refer to this radiation as the synchrotron Čerenkov radiation and the synchrotron radiation in a medium, respectively. In the language of source theory [11], the description of the so-called synchrotron Čerenkov radiation in Ref. [11] is restricted to the case of electron circular motion in the plane perpendicu-

lar to the direction of the uniform magnetic field. The emphasis in the numerical examples is on the case of index of refraction less than unity; this leads to suppression of the very short-wavelength radiation. Because the electron does not propagate parallel to the magnetic field, the helical Čerenkov effect as such is not achievable.

The treatment of the so-called synchrotron radiation in a medium done by Kroll [12] is purely classical. The power spectrum is defined through the Poynting vector which is subsequently rewritten in terms of the electron current density. This, in turn, is expanded in terms of the Bessel functions, their first derivatives, and the δ functions. The power spectrum is given for the infinite interaction time $T \to \infty$ from the beginning. However, the radiation kinematics of the vacuum branch and the forward and backward Čerenkov branches are not identified. As a consequence, the helical Čerenkov effect, which occurs where the forward and backward Čerenkov branches meet, is also not identified in Ref. [12].

Although the expressions for power spectra in both Refs. [11] and [12] contain the Bessel functions and their first derivatives, the comparison with our expression for the power spectrum, relations (36) and (37), is rendered very difficult. This we attribute to the fact that, in deriving the expression for the power spectrum, unlike in Refs. [11] and [12], we utilized the photon circular polarization unit vectors which should be natural in this problem because of the electron helical motion.

[1] J. Šoln, Phys. Rev. D **18**, 2140 (1978).
[2] J. Šoln, J. Appl. Phys. **51**, 5523 (1980).
[3] J. Šoln, J. Appl. Phys. **67**, 3971 (1990); Phys. Rev. A **39**, 3498 (1989); J. Appl. Phys. **58**, 3314 (1985).
[4] W. W. Zachary, Phys. Rev. D **20**, 3412 (1979).
[5] J. Schwinger, Phys. Rev. **75**, 1912 (1949).
[6] G. A. Schott, *Electromagnetic Radiation* (Cambridge University Press, Cambrdige, 1912).
[7] E. Fermi, Phys. Rev. **57**, 485 (1940).
[8] M. Huybrecht and M. Schoenberg, Nuovo Cimento **9**, 764 (1952).
[9] V. P. Zrelov, *Cherenkov Radiation in High-Energy Physics, Part I* (Atomizdat, Moscow, 1968) (translated by the Israel Program for Scientific Translations, Jerusalem, 1970), pp. 19–26.
[10] J. V. Jelley, *Čerenkov Radiation and its Applications* (Pergamon, New York, 1958).
[11] J. Schwinger, W. Tsai, and T. Erber, Ann. Phys. (N.Y.) **96**, 303 (1976).
[12] N. Kroll, in *Free-Electron Generators of Coherent Radiation,* edited by S. F. Jacobs, H. S. Pilloff, M. Sargent III, M. O. Scully, and R. Spitzer, Physics of Quantum Electronics Vol. 7 (Addison-Wesley, London, 1980), pp. 355–375.